Structural, electrical and photovoltaic characteristics of n- ZnSe/p-Ge heterojunctions

M. FADEL[a], A. A. M. FARAG[b*]
[a]*Semiconductor Laboratory, Physics department, Faculty of Education, Ain Shams University, Cairo, Egypt.*
[b]*Thin Film Laboratory, Physics department, Faculty of Education, Ain Shams University, Cairo, Egypt.*

A high quality n-ZnSe/p-Ge heterojunction is produced by Metal organic chemical vapor deposition (MOCVD) technique. The devices structure were investigated by X-ray diffraction and scanning electron microscopy. The devices have good reproducibility of their electrical characteristics and high rectification ratio. The electrical and photovoltaic properties of n-ZnSe/p-Ge heterojunction were investigated by measuring current density-voltage (J-V) and capacitance-voltage (C-V) characteristics at various temperatures and under light illumination of 80 mW/cm^2. The analysis of dark current -voltage characteristics in the temperature range 300-400 K were presented in order to elucidate the conduction mechanisms and to evaluate the device parameters. The charge transport conduction mechanism in the forward biased condition in the low voltage region is described by the modified Schockley effect. For high biases , V≥ 0.6 V , the dark current is a space charge limited current (SCLC) controlled by a single dominant trap level. The capacitance of the device was measured as a function of applied voltage at a frequency of 1MHz, at temperatures ranging from 300 to 400 K, indicating the formation of p-n junction between ZnSe and Ge and the built-in potential was found to decrease with the increase in temperature. The photovoltaic characteristics of the device based on an efficient donor/acceptor combination of n-ZnSe/p-Ge heterojunctions were also studied.

(Received May 3, 2011; accepted August 10, 2011)

Keywords: ZnSe/Ge, Heterojunctions, MOCVD, Photovoltaic

1. Introduction

Semiconductor heterojunctions (HJs) have been widely applied in modern solid state electronic devices [1]. There are growing interests in the HJs and superlattices concerning II-VI compound semiconductors because their band gaps differ by a large amount,which may be used for the design of optoelectronic devices operating in the blue wave length range [2] The wide band gap II–VI semiconductor ZnSe is facing the opportunities and challenges in applying to opto-electronic devices and can be used for building blue laser and light-emitting diodes [3,4]. To build such devices, GaAs wafers have been used as substrates to grow the ZnSe layers. GaAs substrates were favored, mainly, because it is almost lattice-matched to ZnSe. Ge wafers, however, can be used as an alternative to GaAs wafers. Ge wafers, in addition to being almost lattice-matched to ZnSe material, can be less costly than GaAs wafers. Moreover, ZnSe/Ge heterostructures can be used to build high-performance bipolar and field effect transistors. For example, an n-ZnSe/p-Ge heterojunction bipolar transistor (HBT) [5] is expected to have high injection efficiency as well as low base resistance. The high injection efficiency would be due to the large band gap discontinuity between ZnSe and Ge [6,7]. The low base resistance is due to the high mobility of holes in Ge. ZnSe/Ge can also be used to build high-electron-mobility transistors (HEMTs) with high swing voltage [8] and low gate capacitance. Low gate capacitance will be realized because the dielectric constant of ZnSe is 25% lower than that of GaAs or Si [8].

Several researchers have studied ZnSe/Ge heterostructures. Park [9] have grown ZnSe on (1 0 0)Ge substrates using molecular beam epitaxy,MBE. They found that the best material properties were obtained when the substrate temperature was set to 310–350 °C, and Zn to Se beam pressure ratio was around unity. Yamaguchi et al. [10] have reported the growth of a single crystal of ZnSe on (1 0 0) Ge substrate. Kleiman et al. [11] have prepared ZnSe/Ge heterostructures by molecular beam epitaxy. They found that this structure have been characterized by ‘‘full rotation’’ double crystal rocking curve x-ray analyses with particular emphasis placed on the measurement of tilt between the (400) planes of ZnSe and Ge. It was found that the value of the tilt angle between such planes depends on both the epilayer thickness and the orientation of the substrate plane. They have also reported that steps on the substrate surface are shown to be responsible for a redistribution of the bond lengths between the atoms of the substrate and the epilayer in the interface region leading to the formation of tilt between the planes in the epilayer and the substrate. Vinogradov et al. [12] studied the relaxation of trapping sites in ZnSe films in Au-ZnSe/Ge structures, where they observed hole trapping centers in the ZnSe film. Ferraz and Srivastava [13] investigated, theoretically, the atomic relaxation and electronic states in ultra-thin ZnSe/Ge superlattices, using a self-consistent semi-empirical method. They found that ZnSe/Ge superlattice structures (SLS) behave in a similar

way as ZnSe/GaAs SLS. Maung and Williams [14] grew ZnSe layers on top of (1 1 1)Ge wafers, using atmospheric pressure metal-organic chemical vapor deposition (AP-MOCVD). The layers grown, however, were not high-quality crystals. Pan et al. [1] have prepared an ultrathin intralayer of ZnSe at the Si/Ge(111) heterojuncdon with a view to modifying the interfacial properties.Maung and Williams[9] grew ZnSe layers on top of (1 1 1)Ge wafers, using atmospheric pressure metal-organic chemical vapor deposition (AP-MOCVD). The layers grown, however, were not high-quality crystals.Abdel-Motaleb et al. [15] have reported the grown of ZnSe on (1 0 0)p-Ge substrates using atmospheric pressure metal-organic chemical vapor deposition (AP-MOCVD). They grown ZnSe on (1 0 0) p-Ge substrates using atmospheric pressure metal-organic chemical vapor deposition (AP-MOCVD). The quality of the grown materials has been investigated using the atomic force microscope (AFM). This study has shown that high-quality ZnSe materials can be deposited on p-Ge wafers if pre-growth surface treatment is performed. In this work, the present communication deals with the designing of n-ZnSe/p-Ge using MOCVD technique for the first time and characterization of this heterojunction. The electronic parameters that control the device performance, such as barrier height, ideality factor, series resistance and shunt resistance were evaluated from the dark current density – voltage characteristics. Also, the capacitance–voltage characteristics was studied to give information about the type of this heterojunction. Moreover, photovoltaic parameters were extracted from the J–V characteristics under illumination of 80 mW/cm^2.

2. Experimental procedures

The epitaxial layer of ZnSe were grown on p-type Ge (111) substrates using a MOCVD system with a horizontal reactor founded in University of Manchester Institute of Science and Technology UMIST, UK. Diethylzinc (DEZn) was used as the source for Zn, selenium hydride (H2Se) was used as the source Se [15,16]. Both these source gases were diluted in H2. Just prior to growth, the Ge(111) substrate was carefully etched to remove its surface residue oxide. After this treatment, the substrate was mounted in the reactor and cleaned by the H-radicals at 650°C. The substrate temperature was lowered to the deposition temperature and the growth of ZnSe film was started by introducing diethylzinc. Finally the growth was resumed for the desired ZnSe epilayer. The detailed information on the heterojunction preparation by MOCVD were stated elsewhere by Fadel and Farag [16].

The structural characterizations of n-ZnSe/p-Ge heterojunction was investigated using X-ray diffraction pattern. A Philips X-ray diffractometer, model X·Pert, was used for the measurement of utilized monochromatic CuK_α radiationoperated at 40 kV and 25 mA. Scanning electron microscopy, SEM (Model JXA 8400, JEOL, Japan)was used to record the scanning electron micrograph images of the n-ZnSe/p-Ge heterojunctions.

For the J–V measurements, stabilized power supply and high-impedance keithley 617 electrometer were used. The dark C–V measurements were performed at different temperatures using a computerized capacitance–voltage system consisting of C–V meter (model 4108, Solid State Measurement, Inc., Pittsburg). The temperature of samples was measured during electrical measurements by NiCr–NiAl thermocouple with accuracy ±1 K. The J-V characteristics were also investigated under different illumination using 500 W tungsten halogen lamp measurements. The intensity of light was measured by a solar power meter.

3. Results and discussion

3.1 Structure characterizations

Fig. 1 shows the X-ray diffraction patterns of the grown n-ZnSe on p-Ge single crystal . Only two nearest peaks are observed related to ZnSe and Ge with the same (111) orientation . The comparatively higher peak intensity oriented confirms the monocrystalline cubic structure of the Ge substrate while the other belongs to the monocrystalline cubic ZnSe epilayer (according to JCPDS card No.37-1463). It is clearly confirmed that the gowth of ZnSe film on Ge single crystalline substrate by MOCVD yields a good crystalline film and the heterojunction can be used to fabricate high quality optoelectronic devices.

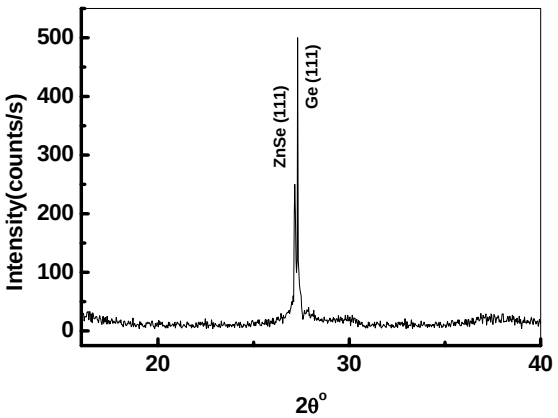

Fig. 1. XRD of n-ZnSe/p-Ge haeterojunction.

The surface topography of the epilayer of n-ZnSe grown on p- Ge substrate by MOCVD was examined by SEM. It is clear from the SEM micrograph, shown in Fig. 2, that fine crystallites characterized by a nearly homogeneous distribution are epitaxially grown which may correspond to the n-ZnSe epilayer.

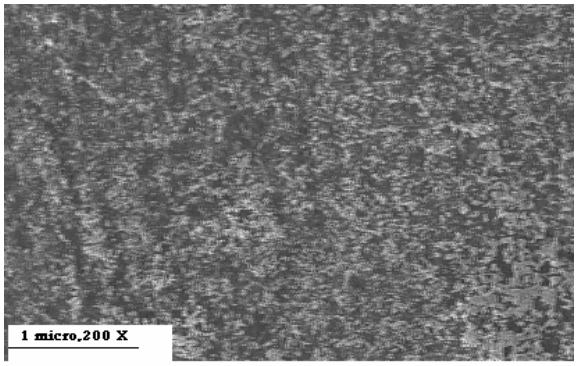

Fig. 2. SEM of n-ZnSe/p-Ge haeterojunction.

3.2 Dark current density–voltage characteristics

Fig. 3 shows the forward and reverse current density–voltage (J-V) characteristics of the n-ZnSe/p-Ge heterojunctions in the temperature range 300-400 K. Measurements of the main heterojunction properties indicate high uniformity of electrical characteristics with a variation in the parameters of less than 5%. Good rectifying property was observed. The rectification ratio, RR, of the device, the ratio of forward current and reverse current at the applied voltage of ±1 V was listed in Table 1. The achievement of such values on the n-ZnSe/p-Ge heterojunctions strongly indicate the high quality of the n-ZnSe film as well as a good characteristics of the n-ZnSe/p-Ge interfaces.

For a detail analysis of J–V curves with respect to conduction mechanisms through the n-ZnSe/p-Ge heterojunctions and device parameters, firstly we found out the implication of Schockley mechanism by seeking out the linear region in the semilogarithmic scale of J–V plot of the forward current–voltage characteristics of the device. The semilogarithmic plot for the device is shown in Fig. 3 shows two distinct regions characterise these curves indicating different conduction mechanisms within the narrow low forward voltage ($0 < V \leq 0.30$ V) and $0.6 \leq V \leq 1.5$ V, respectively. It is known that for a Schockley diode having high series resistance and small shunt resistance, the semilogarithmic J-V plot contains a linear region only in a small range of moderate voltage, while at higher voltages, a downward curved region exist. That is why; we consider that the forward characteristics of the device up to 0.6 V can be fitted well by the modified Schockley equation [17]

$$J=J_0\{exp[q(V-JR_s)/nkT]-1\}+(V-JR_s)/R_{sh} \quad (1)$$

where J_0, n, R_s and R_{sh} are the reverse saturation current, diode ideality factor, series and shunt resistance, respectively, and q is the electronic charge. The source of the series resistance R_s is mostly the combined effect of bulk of organic layers of the device and the barrier. The values of R_s and R_{sh} are determined as follows:
From the Eq. (1), the junction resistance R_J is

$$R_J=dV/dJ = R_s + 1/[\beta(J_0\, exp(V-JR_s)+1/R_{Sh})] \quad (2)$$

where $\beta=q/nkT$.

At higher forward bias region , where R_s affects the curves, Eq. (1) can be approximated as $J=J_0\, exp[\beta(V-IR_s)]$, and since $1/R_{sh} < I$, Eq. (2) can be written as follows:

$$R_J = R_s + 1/\beta J \quad (3)$$

Thus, by plotting R_J versus $1/J$, as shown in Fig. 4, at high forward biases, one can obtained R_J and the value of n .

At low voltage region, where the approximation $\beta J_0 \exp[(V-JR_s)] \ll 1/R_{sh}$ is valid and Eq. (2) becomes

$$R_J=R_s+R_{sh} \quad (4)$$

Usually $R_s \ll R_{sh}$, R_J, thus, approaches R_{sh} at low biases. According to Fig. 4, one can divide the plot into two regions A and B for high and low forward currents, respectively. For region A, it is found that R_J as a function of $1/J$, shows linearity from 0.6 up to 1.5 V (the voltage from J–V plots in Fig. 3, corresponding to the value 4896 Ω of R_J) and after that, the curve deviates from straight line at high forward biases. This fact may suggest that the modified Shockley equation is valid up to 0.6 V and there may be other conduction mechanism taking place for higher values. From the extrapolated linear region A, the determined value of R_s is listed in Table 1. The value of R_{sh} obtained from the region B is also listed in Table 1 at different temperatures in the range 300-400 K. These values of R_s and R_{sh} depending upon experimental conditions are comparable to those obtained by other authors [5-7].

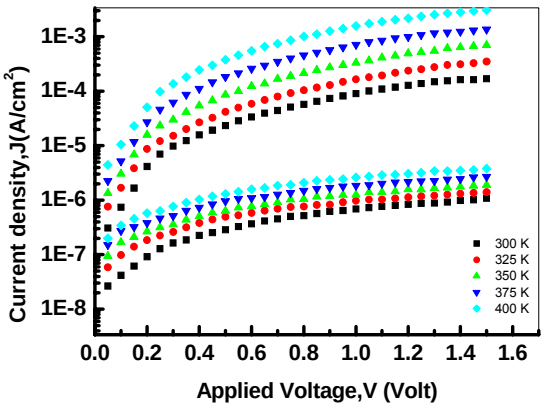

Fig. 3. J-V characteristics of n-ZnSe/p-Ge haeterojunction at different temperatures.

Table 1. Parameters obtained from J-V characteristics.

T(K)	RR(at ±1 V)	R_s(kΩ.cm^2)	R_{sh}(kΩ.cm^2)	n	J_0(A/cm^2)
300	130	4.9	117	2.9	3.1×10^{-7}
325	170	2.15	60	2.6	7.6×10^{-7}
350	260	1.08	37	2.3	1.35×10^{-7}
375	380	0.547	22	2.1	2.25×10^{-7}
400	600	0.242	10	1.9	4.4×10^{-7}

The obtained values of n and reverse J_0 obtained from the slope and intercept of Fig. 3 are listed in Table 1. The value of diode quality factor is greater than unity indicates the presence to a large number of defects at interface between ZnSe and Ge which facilitate the electron–hole recombination.

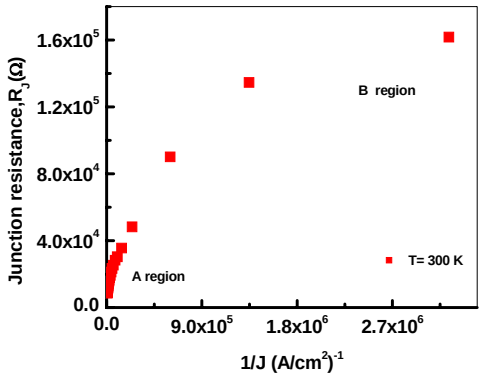

Fig. 4. Junction resistance vs. 1/J for n-ZnSe/p-Ge haeterojunction.

The variation in the semilogarithmic plot of J_o versus $1/T$ given in Fig. 5 follows the form [18]

$$J_o=J_{oo}\exp(-\Delta E/kT), \quad (5)$$

where J_{oo} is a constant. The activation energy ΔE calculated from the slope of the linear fit of Fig. 5 was found to be 0.27 eV. The built-in voltage V_b calculated from the relation, $V_b= n.\ \Delta E/q$ [18] was 0.59 V at 300 K.

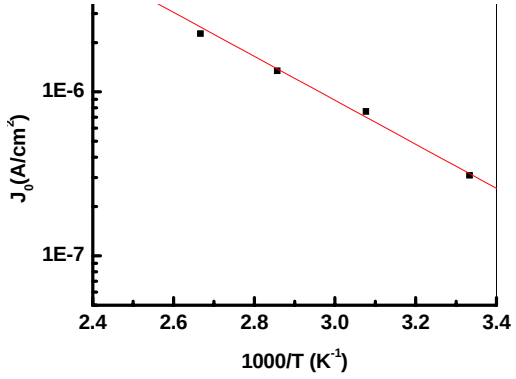

Fig. 5. J_0 vs 1/T for n-ZnSe/p-Ge haeterojunction.

For biases ≥0.6 V, other conduction mechanism seems to be operative. We observed that the current shows a power dependence of voltage, i.e. follows the relation $I\propto V^m$ where $m\approx 2$ as seen from the log (J)–log (V) plot in Fig. 6. this behaviour shows that the forward biased current is space charge limited conduction,SCLC controlled by a single dominant trap level. This behaviour can be expressed by the following equation [19]

$$J= (8/9)\ \varepsilon\mu\ (N_c/N_t)(V^2/d^3)\exp[-(E_c-E_t)/kT] \quad (6)$$

where ε is the permittivity of the ZnSe layer which is taken as 8.07×10^{11} F/m [12], μ is the mobility of electrons, N_t is the total trap concentration and E_c- E_t is the is the difference between the Fermi level and trap level. The value of E_c- E_t can be obtained from the slope of the semilogarithmic plot of J versus 1000/T in the SCLC region, i.e., at voltage 1.3 V (the inset of Fig. 6), and was found to be 0.29 eV.

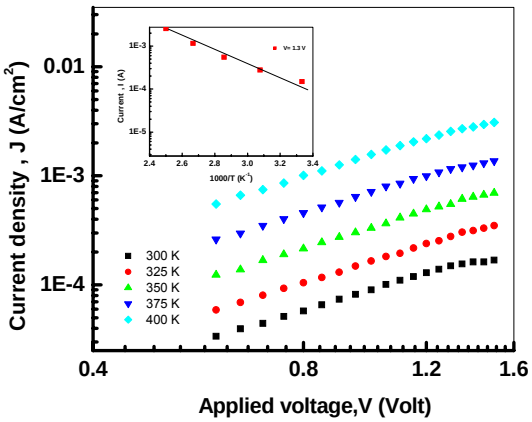

Fig. 6. J-V characteristeristics in log-log scale under high forward bis V ≥ 0.6 V. The inset shows the temperature dependence of current density at 1.3 V.

3.3 Dark capacitance–voltage characteristics

The capacitance of the device was measured as a function of applied voltage at a frequency 1MHz, at temperatures in the range 300 - 400 K. A plot of $1/C^2$ versus applied voltage at different temperatures is shown in Fig. 7. According to the Anderson model, the differential capacitance over the linear portion can be related to applied voltage by equation [20]:

$$1/C^2= 2[(\varepsilon_n N_a+\varepsilon_p N_d)^2(V_b+V)]/[\varepsilon_n N_d+\varepsilon_p N_a)\varepsilon_n\varepsilon_p\varepsilon_0 q N_a N_d A^2 \quad (7)$$

Where ε_n and ε_p are the dielectric constants of the n-type ZnSe and p-type Ge semiconductors, N_d and N_a are the concentrations of ionized donor and acceptor atoms, V_b is the built-in potential, V is the applied voltage and A is the effective area of the device. When $1/C^2 = 0$, V= V_b and when V= 0, the capacitance per unit area is equal to

$$\varepsilon_n\varepsilon_p\varepsilon_0/(\varepsilon_p X_n+\varepsilon_n X_p) \quad (8)$$

Where X_n , X_p are the depletion width of n-type and p-type ZnSe and p-type Ge semiconductors, respectively. For the analysis, we have assumed that, $\varepsilon_n = \varepsilon_p$, = 10, and then the slope of the 1 / C^2-V plot is equal to

$$2(N_a+N_d)/\varepsilon\varepsilon_0 q N_a N_d \quad (9)$$

And then, the values of the X_n, and X_p, are given by [22]

$$X_n=[2N_a\varepsilon V_b/qN_d(N_a+N_d)]^{1/2} \quad (10a)$$

$$X_p=[2N_d\varepsilon V_b/qN_a(N_a+N_d)]^{1/2} \quad (10b)$$

From Fig. 7, the intercept on the voltage axis gives the built-in potential (V_b) which is listed in Table 2. From the slope of the l/C^2-V plot along with Eqs. (7)-(10) and employing N_a=2.3 × 10^{15} cm^{-3} for Ge [23], the values of N_d, X_n, and X_p, have been derived and complied in Table 2 at various temperatures. The values of X_n, X_p, and V_b are invariant with temperature. The value of V_b is equivalent to the difference in the Fermi energies of the two solids before contact [18]. Thus, a material that displays n-type photoconductivity, such as ZnSe, contains a large number of filled traps distributed in the band gap. Holes injected from Ge into ZnSe are rapidly trapped because of their low mobility. However, the p-type Ge is expected to contain a small number of traps distributed at low lying energies in the bandgap.

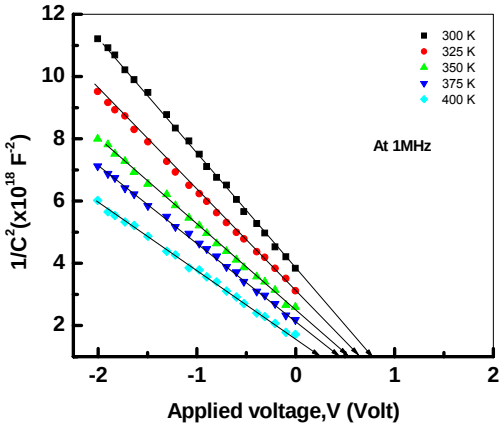

Fig. 7. C^{-2} vs. V at different temperature for n-ZnSe/p-Ge haeterojunction.

Table 2. Parameters obtained from J-V characteristics.

T(K)	V_b(V)	N_d(cm^{-3})	X_n(nm)	X_p(nm)
300	0.74	$3x10^{14}$	140	200
325	0.62	$6×10^{14}$	130	172
350	0.51	$8×10^{14}$	125	160
375	0.39	$2×10^{15}$	119	142
400	0.22	$6×10^{15}$	110	130

3.4. Photovoltaic characteristics of n-ZnSe/p-Ge heterojunctions

Fig. 8 shows the *J–V* characteristics of n-ZnSe/p-Ge heterojunctions devices under illumination of 80 mW/cm^2. The device exhibits a short-circuit current density (J_{SC}) of 17.5 mA/cm^2, an open-circuit voltage (V_{OC}) of 0.5 V, and a fill factor (FF) of 39%. The high short circuit current indicates reduced recombination loss and high shunt resistance (R_{SH}) of the device [22]. These may be due to a good morphology and high charge carrier mobilities of both the p- and n-channel of the devices. For further clarification, the precise measurement of all solar cell parameters have been made by analysing the *J–V* curve, shown in Fig. 8 under 80 mW/cm^2 illumination. Shunt resistance (R_{SH}) has been independently derived from the slope of the *J–V* curve at $J = J_{SC}$ *(V = 0).* Fig. 8 also show the experimental data together with the calculated R_{SH} of the device. Other parameters have been estimated from the y-intercept and the slope of the plot of *(dV/dJ)* as a function of $\{q/nkT\ (J+J_L)^{-1}\}$, as shown in Fig. 9. The plot of *(dV/dJ)* exhibits a good linearity in agreement with the model [24]. The device shows a series resistance (R_S) of 1080 Ω cm^2 and a shunt resistance (R_{SH}) of 100 kΩ. cm^2. The obtained value of R_s under illumination condition was found to be reduced by 22% as compared to that obtained in dark condition. This confirms the improvement of the device under illumination which gives validity in the application of solar cells.

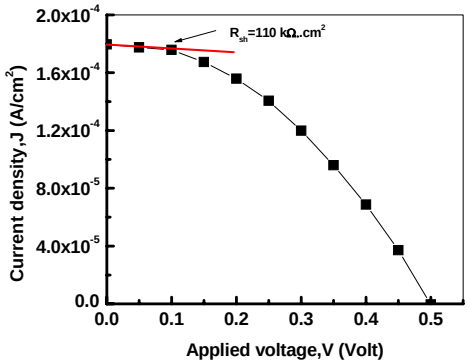

Fig. 8. Illuminated J-V characteristics under 80 mW/cm^2.

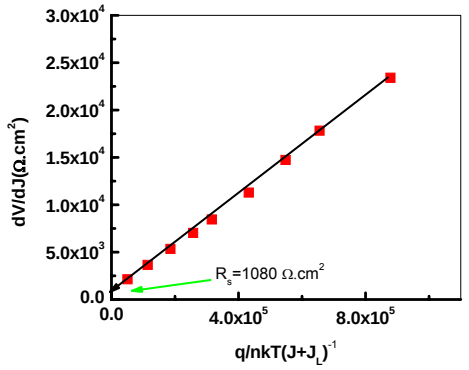

Fig. 9. dV/dJ vs. $q/nkT(J+J_L)^{-1}$ for n-ZnSe/p-Ge haeterojunction.

4. Conclusion

From the *J–V* characteristics, it was found that the device shows the rectification effect which is due to the formation of barrier formed between the epilayer of ZnSe and Ge substrate. The diode quality factor of the device is greater than unity indicates to a large number of defects at the interface between ZnSe and Ge which facilitate the electron–hole recombination in the depletion region. The charge transport conduction mechanism in forward biased condition was described by the modified Schockley effect at low voltage region. For biases >0.6 V, the dark current is a space charge limited current (SCLC) in the presence of single distributed trap. The C–*V* characteristics at 1MHz plots also indicate an abrupt heterojunction formation. The built-in potential and width of depletion region were found to decrease with the increase in temperature. The most promising point with this donor/acceptor combination is that the device exhibits efficient light harvesting throughout the visible region of the solar spectrum.

References

[1] M. Pan, S. P. Wilks, P. R. Dunstan, M. Pritchard, R. H. Williams, D. S. Commack, S. A. Clark, Thin Solid Films **343**, 605 (1999).
[2] F. Yang, D. Ban, R. Fang, S. Xu, P. Xu, S. Yuan, J. Electron Spctroscopy &Related Phenomena **80**, 193 (1996).
[3] Z. Yu, J. Ren, Y. Lansari, B. Sneed, K. Bowers, C. Boney, D. Eason, R. Vaudo, K. Gossett, J. Cook, J. Schetzina. Jpn. J. Appl. Phys. **32**, 663 (1993).
[4] H. Jeon, J. Ding, A. V. Nurmikko, W. Xie, M. Kobayashi, R. L. Gunshor, Appl. Phys. Lett. **60**, 892 (1992).
[5] H. Tseng, J. Shen, R. Hsieh, Jpn. J. Appl. Phys. **33**, L1759 (1994).
[6] B. J. Streetman. Solid State Electronic Devices (4th edition ed.), Prentice-Hall, Englewood Cliffs, NJ (1995).
[7] R. Eppenga. Phys. Rev. B **40**, 10402 (1989).
[8] F. C. Jain. J. Vac. Sci. Technol. B **13**, 661 (1983).
[9] R. M. Park, H. M. Mar, J. Mater. Res. **1**(4), 543 (1986).
[10] E. Yamaguchi, I. Takayasu, T. Minato, M. Kawashima, J. Appl. Phys. **62**, 885 (1987).
[11] J. Kleiman, R. M. Park, H. A. Mar, J. Appl. Phys. **64**, 1201 (1988).
[12] S. Vinogradov, O. Malinovskaya, A. Tolokonnikov. Phys. Stat. Sol. *A* **111**, 201 (1989).
[13] A. Ferraz, G. Srivastava. Semicond. Sci. Technol. **8**, 67 (1993).
[14] N. Maung J. Williams, Chemtronics **3**, 206 (1998).
[15] I. M. Abdel-Motaleb, S. Pal, P. Desai, Journal of Crystal Growth **217**, 366 (2000).
[16] M. Fadel, A. A. M. Farag, J. Optoelectron. Adv. Mater. **11**, 571 (2009).
[17] Kh. S. Karimov, M. M. Ahmed, S. A. Moiz, M. I. Fedorov, Solar Energy Materials &Solar Cells, **87**, 61 (2005).
[18] H. Bayhan, C. Ercelebi, Semicond. Sci.Technol.**12**, 600 (1997).
[19] M. S. Roy, G. D. Sharma, S. G. Sangodkar, Synthetic Metals **81**, 15 (1996).
[20] F. J. Kampas, M. Gouterman, J. Phys. Chem. **81**, 690 (1977).
[21] S. J. Fonash, Solar Cell Devices Physics, Academic Press, London, 92 (1981).
[22] A. Moliton, J. M. Nunzi, Polym. Int. **55**, 583 (2006).
[23] I. M. Abdel-Motaleb, S. Pal, P. Desai, J. Crys. Growth **217**. 366 (2000).
[24] K. Ishibashi, Y. Kimura, M. Niwano, J. Appl. Phys. **103**, 094507 (2008).

*Correspoonding author: alaafaragg@yahoo.com